LLNL-JRNL-636592

Performance of High-Convergence, Layered DT Implosions on Power-Scaling Experiments at National Ignition Facility

V. A. Smalyuk, T. Doeppner, J. L. Kline, T. Ma, H. S. Park, L. J. Atherton, L. R. Benedetti, R. Bionta, D. Bleuel, E. Bond, D. K. Bradley, J. Caggiano, D. A. Callahan, D. T. Casey, P. M. Celliers, C. J. Cerjan, D. Clark, E. L. Dewald, S. N. Dixit, D. H. Edgell, J. Frenje, M. Gatu-Johnson, V. Y. Glebov, S. Glenn, G. Grim, S. W. Haan, B. A. Hammel, E. Hartouni, R. Hatarik, S. Hatchett, D. Hicks, W. W. Hsing, N. Izumi, O. S. Jones, M. H. Key, S. F. Khan, J. D. Kilkenny, J. Knauer, G. A. Kyrala, O. L. Landen, S. Le Pape, B. J. MacGowan, A. J. Mackinnon, A. G. MacPhee, J. McNaney, N. B. Meezan, J. D. Moody, A. Moore, M. Moran, A. Pak, T. Parham, P. K. Patel, R. Petrasso, J. E. Ralph, S. P. Regan, B. A. Remington, H. F. Robey, J. S. Ross, B. K. Spears, et al.

May 14, 2013

Physical Review Letters

Performance of High-Convergence, Layered DT Implosions in Power-Scaling Experiments at the National Ignition Facility

V. A. Smalyuk,[1] T. Döppner,[1] J. L. Kline,[2] T. Ma,[1] H.-S. Park,[1] L. J. Atherton,[1] L. R. Benedetti,[1] R. Bionta,[1] D. Bleuel,[1] E. Bond,[1] D. K. Bradley,[1] J. Caggiano,[1] D. A. Callahan,[1] D. T. Casey,[1] P. M. Celliers,[1] C. J. Cerjan,[1] D. Clark,[1] E. L. Dewald,[1] S. N. Dixit,[1] D. H. Edgell,[3] J. Frenje,[4] M. Gatu-Johnson,[4] V. Y. Glebov,[3] S. Glenn,[1] G. Grim,[2] S. W. Haan,[1] B. A. Hammel,[1] E. P. Hartouni,[1] R. Hatarik,[1] S. Hatchett,[1] D. G. Hicks,[1] W. W. Hsing,[1] N. Izumi,[1] O. S. Jones,[1] M. H. Key,[1] S. F. Khan,[1] J. D. Kilkenny,[5] J. Knauer,[3] G. A. Kyrala,[2] O. L. Landen,[1] S. Le Pape,[1] B. J. MacGowan,[1] A. J. Mackinnon,[1] A. G. MacPhee,[1] J. McNaney,[1] N. B. Meezan,[1] J. D. Moody,[1] A. Moore,[1] M. Moran,[1] A. Pak,[1] T. Parham,[1] P. K. Patel,[1] R. Petrasso,[4] J. E. Ralph,[1] S. P. Regan,[3] B. A. Remington,[1] H. F. Robey,[1] J. S. Ross,[1] B. K. Spears,[1] P. T. Springer,[1] L. J. Suter,[1] R. Tommasini,[1] R. P. Town,[1] S. V. Weber,[1] K. Widmann,[1] J. D. Lindl,[1] M. J. Edwards,[1] S. H. Glenzer,[1] and E. I. Moses[1]

[1]Lawrence Livermore National Laboratory, Livermore, CA 94550

[2]Los Alamos National Laboratory, Los Alamos, NM 87545

[3]Laboratory for Laser Energetics, University of Rochester, Rochester, NY 14623

[4]Massachusetts Institute of Technology, Cambridge, MA

[5]General Atomics, San Diego, CA

ABSTRACT

Experiments with lower power, extended-duration drives were performed to study the sensitivity of implosion performance to the peak power of the drive using x-ray driven capsules containing cryogenic DT layers surrounded by plastic ablators on the National Ignition Facility. Peak laser power was varied from ~290 to ~400 TW with total energies in the range from ~1.5 to ~1.7 MJ. Highest performance with ignition threshold factor (ITFX) of ~0.1 and a fuel areal density of ~1.3±0.1 g/cm^2 was achieved at peak power of 350 TW, while performance was reduced at both lower and higher powers.

The goal of inertial confinement fusion (ICF) [1,2] is to implode a spherical target to achieve high compression of the fuel and high temperature in the hot spot, to trigger ignition and produce significant thermonuclear energy gain. In indirectly driven laser ignition designs, x-rays produced by the laser in high-Z enclosures (hohlraums) ablate spherical low-Z capsules to implode inner layers of cryogenic DT fuel. The imploded fuel must achieve high temperature (>5 keV) in the central hot-spot, and a central hot-spot with column density ~0.3 g/cm^2 enclosed in a main-fuel layer with ~1.5 g/cm^2. The current point design at the National Ignition Facility (NIF) [3] uses a plastic ablator. It reaches a peak implosion velocity of ~360 km/s, driven with a 1.6 MJ laser pulse at peak power of 410 TW [4]. To achieve high compression, the fuel entropy in the surrounding DT shell must remain low so that it can be compressed to high density with the available energy [2]. The isentrope of the high-density DT entropy is defined [4] by adiabat $\alpha = P / P_{cold}$, the ratio of the plasma pressure P to the Fermi pressure of a fully degenerate gas P_{cold} [4,5]. In the NIF point design, the adiabat α must be as low as ~1.4 to achieve high compression of the surrounding DT fuel with peak fuel areal-density of ~1.4 g/cm^2, peak total shell areal-density of ~1.8 g/cm^2 including the remaining ablator, and the predicted neutron yield of ~20 MJ [4].

In recent cryogenic DT implosions on NIF, the implosion velocities and fuel compressions have been smaller than predictions, to a degree consistent with overall ~15% reduction in x-ray drive [6,7]. The drive deficit appears to have been especially pronounced during a coasting phase after the laser drive was switched off, typically at shell convergence ratio of ~2, corresponding to the time when the outer shell radius was at ~500 μm from the shell center [8,9]. In addition to the reduced velocity, the reduction in the x-ray drive during the coasting phase could lead to shell decompression resulting in lower shell convergence and reduced compression of the DT fuel [9]. This Letter describes results of implosions with new, extended laser drives intended to reduce the duration of the coasting phase, and therefore improve fuel compression. These experiments were based on three power-scaled implosions in which peak laser power was varied from ~290 to ~400 TW with total laser energy from ~1.5 to ~1.7 MJ, for which the pulses were turned off when the outer shell radius was expected to be ~300 μm from the shell center. The main goal of these power-scaling implosions was to improve target compression and study the sensitivity of implosion performance to the peak power of the drive. Higher shell compression was achieved at peak drive power of 350 TW, with highest fuel areal density and ignition threshold factor (ITFX), as introduced in Ref. [5] and defined below. Implosion performance was also observed to have high variability due to drive variations and ablator-fuel mix. The experiments described here are not a large enough data-base to draw firm conclusions about performance scaling and variability, or about the ultimate performance of this target design. They are being published now in order to update the scientific community on the progress of this highly visible inertial fusion program.

These experiments represent the culmination of a campaign that characterized the implosion shock timing and symmetry, as described in Ref. 4. Capsule and hohlraum details were as previously published (Fig.1 of Ref. [6]), with the exceptions that the Si concentration was doubled in all Si-doped layers, and the hohlraums were made of Uranium with a 0.6-μm Au lining. Plastic shells including Si-doped layers had nominal 195-μm thickness and 2280-μm-initial outer diameter, with inner cryogenic DT layer nominal thickness of 69 μm. The U hohlraum produces higher drive at peak power [10,11]. The inner Au layer provides oxidation protection for the U [10,11]. The laser is believed to be absorbed in the Au layer, and does not interact with the U. Details of the laser pulses, pointing, and the hohlraum geometry were ascertained by preliminary experiments as described in Refs 4-12. Figure 1 shows the laser pulses used in three implosions with peak powers of ~290 TW, ~350 TW, and ~400 TW, and total laser energies of ~1.5, ~1.6 and ~1.7 MJ, respectively. Table 1 summarizes measured and predicted drive and performance results. The higher-power pulses were truncated earlier than lower-power pulses, all three being turned off when the outer shell radius was expected to be at ~300 μm from the shell center. All three pulses were intended to be identical before the start of the peak of the drive at ~18 ns, with shock timing optimized by prior "keyhole" experiments [12]. Therefore the fuel adiabats, which are believed to be determined by the timing and strength of the first four shocks, were expected to be the same before peak power [12]. As shown in Table 1, the simulated adiabats in these shots were close to the ignition specification of ~1.4, while for the 400-TW shot it was slightly higher, ~2.0 [13]. All target parameters including initial capsule and ice roughness were also intended to remain constant in these experiments.

The roughnesses of the plastic capsule surfaces and ice layers were comprehensively characterized, and were similar in the three shots. In particular, outer capsule surfaces were similar and met ignition specifications. DT ice roughness power spectra were also similar, and met ignition requirements for all modes except for mode 1 on shot N120321, where it was ~2 times higher than the ignition requirement. The effects of ice surface grooves can be characterized by using a parameter *K*, defined as a sum over all defects with area A and length L as $K = \sqrt{\frac{1}{V_{fuel}} \sum_{i=1}^{n} A_i^2 L_i}$, where V_{fuel} is the volume of the DT fuel [4]. Ignition requirements [5] have been set requiring K<0.70 μm, and the largest groove area A required to be <200 μm^2. For 290-TW, 350-TW, and 400-TW shots, the K values were measured to be 0.77 μm, 0.70 μm, and 0.75 μm, respectively, close to the ignition requirement; the largest groove areas were 166 μm^2, 153 μm^2, and 156 μm^2, respectively, meeting the ignition requirement. The dust particles on outer surface were also characterized. Although ignition specifications required no single particle with a volume greater than 30 μm^3 should be present on a capsule surface [4], each shot had one particle detected that exceeded this limit. While the 350-TW and 400-TW shots had dust particle sizes within a factor of 2 of the ignition requirements, the particle size for 290-TW shot was about 5 times larger than the requirement.

The performance of all three implosions was characterized with a comprehensive set of nuclear and x-ray diagnostics [14,15]. The measured peak temperatures were 296±4 eV, 305±4 eV, and 322±4 eV, for the 290-TW, 350-TW, and 400-TW shots, respectively. X-ray measurements of imploded core emission, with photon energies >8 keV at peak compression, showed good symmetry of the emitting hot-spot, captured using time-resolved framing cameras [16]. The hot-spot distortion requirement was <25% rms [4] for the deviation from round of the emission contour at 17% of the peak brightness. For the 400-TW shot, the measured hot-spot distortion was 12%±1% rms, for the 350-TW shot 16%±4% rms, and for the 290-TW shot 11%±3% rms. The best performing 350-TW shot had the highest asymmetry among the three shots, with largest amplitude being for mode 2 in the polar view, M_2/M_0=0.16±0.02. Fuel compression was inferred using the down-scattered ratio (DSR) of scattered neutrons in the range from 10 to 12 MeV relative to primary neutrons in the range from 13 to 15 MeV [17]. The down-scattered neutrons determining DSR are mostly scattered in the DT fuel, and in simulations DSR is proportional to the fuel areal density [17,18].

Measured implosion bang times were 22.95±0.04 ns, 22.84±0.04 ns, and 22.67±0.04 ns, for the 290-TW, 350-TW, and 400-TW shots, respectively. As expected, bang time was earlier for higher peak pulses. The best nuclear performance was measured for the 350-TW shot with neutron yield of 4.2±0.1 $\times 10^{14}$, ion temperature of 3.1±0.1 keV, and DSR of 6.3±0.5%. Both higher and lower power shots performed worse. Figure 2 shows yield performance of these three implosions as a function of peak intensity. To show a trend and variability, three other similar implosions were added in Fig. 2, although they had some capsule and drive parameters slightly different from the three baseline implosions shown in Table 1. For example, both shots N120316 and N120412 had a small amount of additional Ge dopant, in addition to the nominal Si dopant, with reduced amounts of Si so that the net x-ray absorption is predicted to be the same. Also, N120316 had faster, 2-ns rise of the main pulse, compared to the 3-ns rise used in all other shots from the group. Shot N120417 used a Au hohlraum, while the other shots were with U hohlraums. To compensate for the slightly more efficient U drive, the peak laser power in shot N120417 was 375 TW, and the x-ray drive was similar to the two shots with U hohlraums (N120321 and N120316) driven with 350 TW [11]. Therefore the peak power for the shot N120417 is plotted as 350 TW in Fig. 2 for a fair comparison. The performance was very reproducible in the shots N120321 and N120417, but was reduced ~50% in the shot N120316; this could be a consequence of ~5% power reduction in the beams responsible for equatorial drive. As peak power increased, the yield performance peaked at 350-TW, but it dropped in 400-TW shots.

Figure 3 shows the performance of these three shots in comparison with all other layered DT NIF shots (shown with grey and black colors). Solid and dashed curves are contours of constant ignition threshold factor (ITFX), defined as

$ITFX = (\frac{Y_{DT}}{3.2e15})(\frac{DSR}{0.07})^{2.3}$, where Y_{DT} is the measured DT yield in the primary 13-15 MeV range [4]. In simulations, ITFX is a good measure of how close an implosion is to the threshold for thermonuclear ignition [5]. The 350-TW shot N120321 was the highest performer among all DT shots to date on NIF, with highest DSR, corresponding to the fuel areal density of 1.3±0.1 g/cm^2 and ITFX of ~0.1.

Performance degradation of the 400-TW shot probably resulted from stronger susceptibility to hydrodynamic instability growth. The stronger drive is predicted by simulations to result in relatively larger instability growth at the ablation front, as shown in Fig 4. At the same time, the ablator mass remaining was predicted lower (as shown in Table 1), making it more vulnerable to the hydrodynamic instabilities since the ablation-front modulations have less material to penetrate to reach the core. While nuclear performance was lower, with the neutron yield reduced by a factor of ~3.2, and the ion temperature by a factor of ~1.8, the x-ray brightness was higher in the 400-TW shot, indicating increased ablator mix at peak compression [19,20]. This inferred mass of plastic mixed into the DT hot spot, based on x-ray brightness, neutron yield, and observed temperature, [21,22] was ~4000 ng in the 400-TW shot, compared to 320 ng in the 350-TW shot. While performance degradation at 400-TW was observed with two shots, only one shot was done at lower peak drive of 290 TW, making conclusions about its performance problematic. Ablation-front growth factors were lower and mass remaining higher than in the 350-TW shots, but the measured yield and ion temperature indicate worse performance. The 290-TW shot had the largest foreign particle on the capsule surface with volume of 154 μm^3, about a factor of 5 above ignition requirements, possibly affecting its performance. The amount of inferred plastic mix was ~450 ng. Since the 290-TW implosion was slower, deceleration-phase growth at the inner shell surface might be more important than in higher-power implosions. Additional repeatability shots are required to determine a performance trend at low power.

In Table 1, the experimental results are compared with those predicted by 1D and 2D simulations. Among the three "power-scaling" shots, the highest ratio of the measured neutron yield to that predicted by 1D simulation (yield over "clean" or YOC) was 11% for the 350-TW shot. The 2D simulations include measured surface roughness at all unstable interfaces including the DT ice roughness [9], while they do not include effects of the isolated 3D features including particles at the ablation surface, discussed above. Large deviations of the 2D predictions from the measured results indicate a need for improvements in simulations to make them more realistic. It is important to emphasize the performance variability (~2x in the yield and ~1.5x in the ion temperature) of these high-compression implosions; similar variability was also observed on high-convergence cryogenic implosions at OMEGA [23]. Even at slightly lower compressions, in NIF implosions with measured DSR of ~4.5% [24], the neutron yield was measured to be variable by factors of up to 2.5x. These experiments had nominally the same drive and very similar capsule roughness parameters. In Fig. 4, a pair of nominally the same implosions, shown by two black squares, have a yield variation of ~2x. These shots

(N120126 and N120205, in order of increasing yield) had shorter peak-power pulses (turned off at a capsule radius of 500 μm), with main pulse rise-time of 3-ns, and peak power of 436 TW. Two implosions shown by black triangles (shots N120802, and N111215, in order of increasing yield) had similar conditions but the yield performance varied by a factor of ~2.5. They were also taken at peak power of 436 TW, but with faster rise time of the main pulse of 2 ns. Observed variability makes understanding of high-convergence implosions very challenging, especially because the performance depends on many interdependent parameters.

In conclusion, experiments with an extended-duration drive achieved the highest compression in implosions with x-ray driven CH capsules containing cryogenic DT layers. Peak laser power was varied in the range from ~290 to ~400 TW with total energies in the range from ~1.5 to ~1.7 MJ in a series of three power-scaling implosions. Highest performance with ignition threshold factor (ITFX) of ~0.1 and a fuel areal density of ~1.3 g/cm^2 was achieved in the intermediate power 350-TW shot, while implosion performance at such high compression was shown to have high variability.

This work was performed under the auspices of the U.S. Department of Energy by Lawrence Livermore National Laboratory under Contract DE-AC52-07NA27344.

REFERENCES

[1] S. Atzeni and J. Meyer-ter-Vehn, *The Physics of Inertial Fusion: Beam Plasma Interaction, Hydrodynamics, Hot Dense Matter*, International Series of Monographs on Physics (Clarendon Press, Oxford, 2004).

[2] J. D. Lindl, *Inertial Confinement Fusion: The Quest for Ignition and Energy Gain Using Indirect Drive* (Springer-Verlag, New York, 1998).

[3] E. I. Moses, R. N. Boyd, B. A. Remington, C. J. Keane, and R. Al-Ayat, *Phys. Plasmas* **16**, 041006 (2009); G. H. Miller, E. I. Moses and C. R. Wuest, *Opt. Eng.* **443**, 2841 (2004).

[4] S. W. Haan, *et al*., Phys. Plasmas **18,** 051001 (2011).

[5] B. K. Spears, *et al.*, Phys. Plasmas **19**, 056316 (2012).

[6] S. H. Glenzer, *et al.*, Physics Of Plasmas **19**, 056318 (2012).

[7] D. G. Hicks, *et al*., Phys. Plasmas **17**, 122702 (2012).

[8] D. A. Callahan, *et al*., Phys. Plasmas **19**, 056305 (2012).

[9] D. S. Clark, *et al.*, "Detailed implosion modeling of deuterium-tritium layered experiments on the National Ignition Facility," accepted in Phys. Plasmas.

[10] N. B. Meezan, *et al.*, "X-ray driven implosions at ignition relevant velocities on the National Ignition Facility," accepted in Phys. Plasmas.

[11] J. L. Kline, *et al.*, "Hohlraum Energetics Scaling to 520 TW on the National Ignition Facility," accepted in Phys. Plasmas.

[12] H. F. Robey, *et al.*, Phys. Rev. Lett. **108**, 215004 (2012).

[13] H. F. Robey, *et al.*, "The effect of laser pulse shape variations on the adiabat of NIF capsule implosions", accepted in Phys. Plasmas.

[14] M. J. Edwards, *et al.*, Phys. Plasmas **18**, 051003 (2011).

[15] S. H. Glenzer, *et al*., Phys. Rev. Lett. **106**, 085004 (2011).

[16] S. Glenn, *et al.*, Rev. Sc. Instrum. **83**, 10E539 (2010).

[17] J. A. Frenje, et al., Rev. Sci. Instrum. **79**, 10E502 (2008).

[18] O. S. Jones, *et al.*, Phys. Plasmas **19**, 056315 (2012).

[19] T. Ma, *et al.*, Rev. Sc. Instrum. **83**, 10E115 (2012).

[20] N. Izumi, *et al.*, Rev. Sc. Instrum. **83**, 10E121 (2012).

[21] T. Ma, *et al*., "Onset of Hydrodynamic Mix in High-Velocity, Highly Compressed Inertial Confinement Fusion Implosions", submitted to Phys. Rev. Lett.

[22] B. Hammel, *et al.*, Phys. Plasmas **18**, 056310 (2011).

[23] V. N. Goncharov, *et al.*, Phys. Rev. Lett. **104**, 165001 (2010).

[24] A. Mackinnon, *et al.*, Phys. Rev. Lett. **108,** 215005 (2012).

TABLE CAPTION

Table 1. Key experimental results and predictions using 1D and 2D simulations for shots with peak powers of 290 TW, 350 TW, and 400 TW.

FIGURE CAPTIONS

FIG. 1. Pulse shapes used in "power-scaling" implosion experiments with peak power of 290 TW (shot N120422, dotted curve), 350 TW (shot N120321, solid curve), and 400 TW (shot N120405, dashed curve).

FIG. 2. Yield performance as a function of peak laser power, showing the highest performance achieved at 350 TW.

FIG. 3. Measured DT neutron yield in the range from 13 to 15 MeV plotted against measured neutron down-scattered-ratio DSR for all cryogenic DT implosions on NIF (grey and black colors) and with 290-TW, 350-TW, 400-TW implosions showed in blue, red, and green colors, respectively. Solid curves represent contours of the net performance parameter ITFX ranging from 0.02 to 1. Two black triangles represent implosions with similar conditions, while two black squares represent another pair of similar implosions, as described in the text. The highest ITFX was achieved at peak power of 350 TW.

FIG. 4. Predicted linear growth factors of ablation-front modulations, defined as the perturbation amplitude on the ablation front at peak fuel velocity, divided by initial amplitude, as a function of modulation spherical harmonic mode number for the three indicated drive powers.

Table 1

	N120422, peak power 290 TW			N120321, peak power 350 TW			N120405, peak power 400 TW		
	1-D	2-D	Exp.	1-D	2-D	Exp.	1-D	2-D	Exp.
Fuel velocity (km/s)	301.9	304.2	—	319.7	332	—	340.6	339.9	—
Remaining ablator (%)	13.2	11.7	—	11.8	8.9	—	9	7.5	—
Volume of largest foreign surface particle (μm^3)	—	—	154	—	—	68	—	—	41
Ice defect parameter K (μm)	—	—	0.77	—	—	0.7	—	—	0.75
Fuel adiabat	1.46	1.41	—	1.43	1.46	—	2.1	1.88	—
DSR (%)	6.78	6.76	5.4±0.3	6.44	6.2	6.3±0.5	5.75	5.64	5.1±0.3
Ion temperature (keV)	2.96	2.93	1.8±0.1	3.14	3.21	3.1±0.1	2.99	3.11	1.7±0.1
Neutron Yield (10^{14})	23.3	16.9	0.8±0.02	37	20.9	4.2±0.1	40.9	30.7	1.3±0.03
Measured Yield over prediction (%)	4.3±0.9	4.7±1.2	—	11.4±0.3	20.1±0.5	—	3.2±0.1	4.2±0.1	—

Figure 1

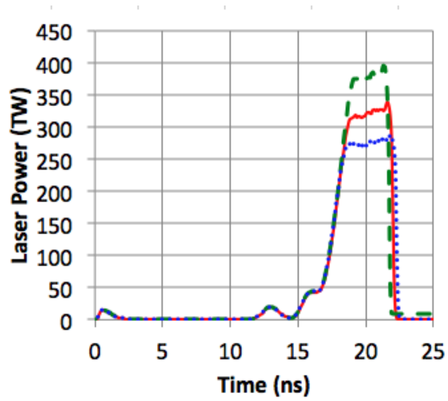

Laser Power (TW)
450
400
350
300
250
200
150
100
50
0
0
5
10
15
20
25
Time (ns)

Figure 2

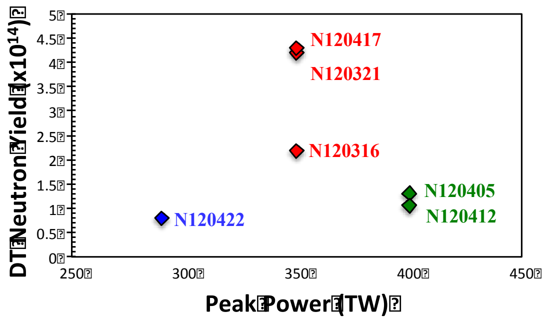
DT Neutron Yield (x10^14)
5
4.5
4
3.5
3
2.5
2
1.5
1
0.5
0
250
300
350
400
450
Peak Power (TW)
N120417
N120321
N120316
N120405
N120412
N120422

Figure 3

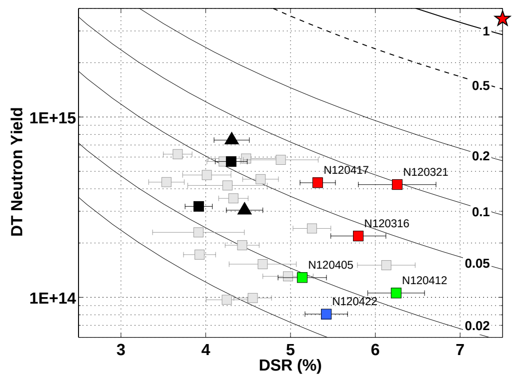

DT Neutron Yield
1E+15
1E+14
DSR (%)
3
4
5
6
7
1
0.5
0.2
0.1
0.05
0.02
N120417
N120321
N120316
N120405
N120412
N120422

Figure 4

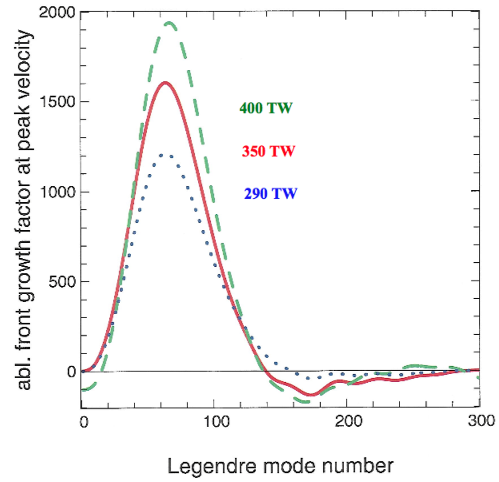

2000
1500
1000
500
0
0
100
200
300
abl. front growth factor at peak velocity
Legendre mode number
400 TW
350 TW
290 TW